Experimental And Theoretical Study on The Impact Strength and Hardness Properties Of HDPE/SWCNTs Nanocomposites

R.T.Tebeta
Mechanical Engineering Science Department, Faculty of Engineering and the Built Environment.
The University of Johannesburg.
Johannesburg 2006, South Africa.
thapelotrt@gmail.com

D.M. Madyira
Mechanical Engineering Science Department, Faculty of Engineering and the Built Environment.
The University of Johannesburg.
Johannesburg 2006, South Africa.
dmadyira@uj.ac.za

A.M. Fatthi
Department of Mechanical Engineering.
Islamic Azad University, Tabriz Branch.
Tabriz, Iran.
fattahi.a@gmail.com

H.M. Ngwangwa
Department of Mechanical Engineering, College of Science, Engineering Technology.
The University of South Africa.
Florida 1710, South Africa.
Ngwanhm@unisa.ac.za

***Abstract*—Polymer-based nanocomposites are widely investigated owing to their unique and remarkable mechanical properties. Yet, obtaining polymer nanocomposites with improved impact strength and acceptable hardness properties is a major challenge. This is because various types of polymers and nanoparticles can be combined to, or sometimes, fail to achieve such properties. However, the use of High-Density Polyethylene (HDPE) reinforced with Single-Walled Carbon Nanotubes (SWCNTs) nanoparticles at various weight fractions was proposed in this work. The analytical study was conducted according to the FEM approach on the hardness properties of HDPE/SWCNTs nanocomposites samples. The analytical FEM results of the hardness properties were validated by experimental results. The experimental study was conducted based on the hardness test and the Charpy impact test. The experimental results obtained showed a significant improvement in the mechanical properties of HDPE reinforced with SWCNTs nanoparticles. At 0.8 wt% of SWCNTs nanoparticles, considerable impact strength and hardness improvement were experienced. The impact strength of the HDPE was enhanced by 62.8%. Moreover, the impact test samples were found to be brittle based on the way they fractured after the test. This was validated using the tensile test results of another study. The hardness properties of HDPE were improved by 20.6%, which was found to be in support of the impact strength and tensile test findings. Furthermore, the theoretical model for the hardness properties of nanocomposites showed to correlate with the obtained results. These results prove that SWCNTs might serve as a suitable strengthening material for various polymers.**

Keywords—Hardness properties, HDPE, Impact strength, Nanocomposites, SWCNTs

I. INTRODUCTION (*HEADING 1*)

The development of new and advanced materials in the lightweight car body industry, wind turbines, aerospace, and other related industries, has attracted the attention of many researchers globally. This is due to the cost-effectiveness of designing lightweight automobiles or airplanes in terms of fuel consumption and energy absorption during collation [1]. Polymer-based nanocomposites have been shown to be better materials that can replace steel, aluminum, and magnesium in the mentioned industries if they are well-improved. The development and investigation of polymer-based nanocomposites have gained popularity these days due to the mentioned motives. Polymer-based nanocomposites have opened a wide range of studies where various types of polymers are reinforced with different kinds of nanoparticles or natural fibers to enhance their mechanical, thermal, creep, fatigue, or other properties. Salah et al, [2]. conducted the experimental investigation on the High-Density Polyethylene (HDPE) reinforced with Carbon nanotubes (CNTs) of oil fly ash. The objective of their study was to examine the effective way of reinforcing thermoplastic-based nanocomposites. Their outputs showed that CNTs of oil fly ash are potential nanoparticles of reinforcing thermoplastics. The used CNTs nanoparticles displayed considerable enhancement in the mechanical properties of HDPE/CNTs nanocomposites as the weight fractions of CNTs increased. At the CNTs weight fractions of 1-2 wt%, their results showed effective improvement in Young's modulus and tensile strength of the nanocomposites by 38% and 20% respectively. Furthermore, their results showed improvement in mechanical properties such as hardness and breaking load. Refiee et al, [3] and Liu et al, [4], used an experimental approach to examine the effect of low Graphene Content on the mechanical properties of epoxy. Their results showed that graphene platelets increased the tensile and Young modulus on epoxy-based nanocomposites. Moreover, Refiee et al, [3]. went further to compare the effect of Single-Walled Carbone Nanotubes (SWCNTs) and Multi-Walled Carbone Nanotubes (MWCNTs) with low graphene content on the mechanical properties of epoxy nanocomposites. The obtained results showed that graphene platelets outperform SWCNTs and MWCNTs nanoparticles in terms of improving fracture toughness, Young's modulus, fracture energy, ultimate

tensile strength, and resistance to fatigue crack propagation of the material. Tebeta et al, [5] used numerical and experimental approaches to investigate the elastic properties of HDPE reinforced with SWCNTs at various weight fractions. In their investigation, they also considered the consequences of two processing methods which are injection and compression molding. The obtained results showed that the addition of SWCNTs nanoparticles weight fractions improves the elastic properties of nanocomposites for both processing methods. Moreover, it was shown that injection molding yields better elastic properties of HDPE/SWCNTs nanocomposites compared to compression molding. More experimental and numerical studies on Polyethylene reinforced with CNTs were made by [6, 7, 8, 9, 10], to demonstrate the effect of CNT nanoparticles on the mechanical properties of nanocomposites by varying the processing parameters or techniques. This shows that the parameters such as the weight fractions of the nanoparticles, processing parameters, processing techniques, and the mixing methods of the nanoparticles with the polymer matrix affect the enhancement of the mechanical properties of the composites. Moreover, researchers such as, [11, 12, 13] further demonstrated that various nanoparticles can be used to enhance the mechanical, and thermal properties of the various polymer. This shows that several studies can be conducted based on enhancing polymer matrix properties using different approaches and a variety of nanoparticles as well as processing techniques.

However, in this work, the hardness properties and the impact strength of HDPE reinforced with SWCNTs nanoparticles are being investigated. SWCNTs nanoparticles were added into the HDPE matrix at the weight fractions of 0 wt%, 0.2 wt%, 0.4 wt%, 0.6 wt%, and 0.8 wt%. The theoretical Finite Element Method (FEM) was implemented to demonstrate the effect of adding SWCNTs nanoparticles on the hardness properties of HDPE/SWCNTs nanocomposites. Theoretical models are widely used to predict or determine various engineering and physics problems, or mathematical concepts, and are regarded as approximating techniques, which can be improved by modifications [14, 15]. The improved or accurate analytical models are good for the investigation because they save time and costs. However, to prove or validate the accuracy of the theoretical models is essential to conduct an experimental investigation. In this work, the experimental procedure was conducted according to the preparation and testing of HDPE/SWCNTs nanocomposites samples through hardness testing and the Charpy impact test. To produce the hardness and the Charpy impact samples of HDPE/SWCNTs nanocomposites according to the stated weight fractions, injection molding processing was used. For testing, a Rockwell hardness tester and the Charpy impact tester were used for hardness and impact strength respectively.

The outline of the manuscript is presented as follows: Section 2 introduced the theoretical RVE and FEM model used to demonstrate the concept of hardness properties of the HDPE/SWCNTs nanocomposites; Section 3 described the experimental hardness test for the validation of the theoretical FEM model and the Charpy impact test for the demonstration of the impact strength of the produced nanocomposites backed up by the tensile test results; Section 4 discusses the theoretical and experimental results; Section 5 concludes.

II. THEORETICAL MODELING

A. *RVE Representation*

This part describes and models the determination of the hardness properties of HDPE/SWCNTs nanocomposites. The hardness of a material is a general term that has various meanings depending on the application or field of study. Typically, hardness in materials science of strength of material means resistance to deformation or it may be described as the resistance to the indentation in the field mechanics of materials [16]. The hardness test on the material can be conducted in different ways using various test methods depending on the material. Since the study in this paper is based on polymer-based nanocomposites which are said to be soft materials compared to metals. Then Rockwell hardness test model is developed to generate a theoretical solution for hardness properties. Figure 1 demonstrates the schematic of the Rockwell hardness test process, where Figure 1 (a) shows the side view of the test sample projected to a load imposed by a steel ball indenter. Figure 1 (b) displays the top view of the test sample after the indentation.

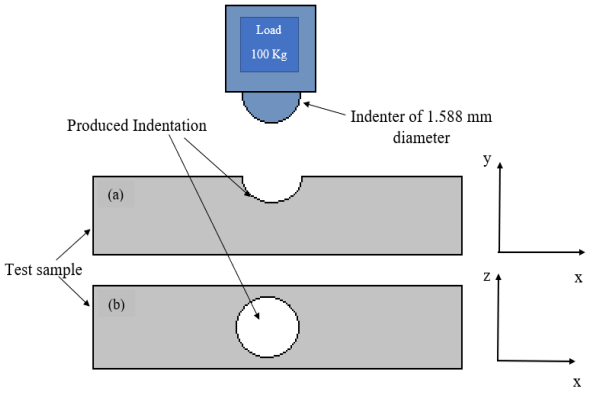

Fig. 1. Steel ball indenter imposed on the test sample

From the schematic of the Rockwell hardness test in Figure 1, the concept of Representative Volume Element (RVE) was developed based on the force acting on the indented section. It is assumed that the steel ball indenter at a given load will compress a sample at a specified area to create an indentation of diameter d and the depth U. Figure 2 presents the dimensions of the indentation created in terms of d as the diameter of the indentation, U as the depth of the indenter (or the deflection of the sample with respect to the test surface from the side view), and D as the diameter of the indenter.

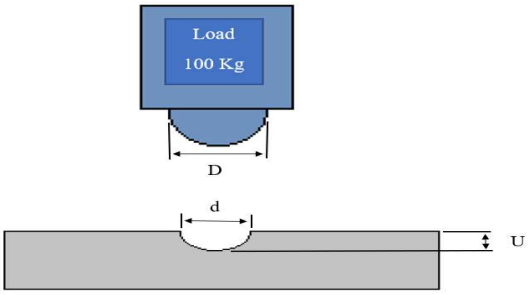

Fig. 2. The dimensions of the indenter and the indentation on the test sample

The Representative Volume Element (RVE) was selected as a small section on the test region of the sample to represent the entire sample behavior under a compression load. Figures 3 (a) and (b) show the HDPE/SWCNTs nanocomposites test samples before and after the indentation, respectively. The effect of indentation of the RVE is shown, where the applied load represents the indenter load, and the fixed region represents the flat bottom plate of the hardness tester. It was also assumed that the forces acting on the test section of the sample are the same forces acting on the RVE as presented in Figure 4.

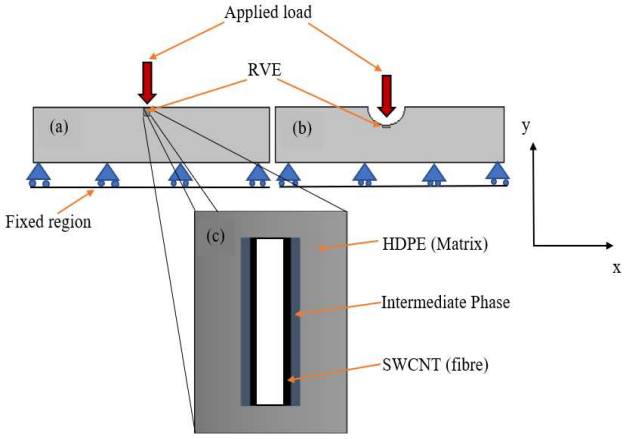

Fig. 3. HDPE/SWCNTs nanocomposites Representative Volume Element (RVE)

Figure 3 (c) demonstrates the RVE with the orientation in which the HDPE matrix, intermediate phase, and SWCNT fiber and aligned. Figure 4 indicates the applied loads and the geometry of the RVE. Figure 4 (a) illustrates the applied load and the fixed region of the RVE in the y-direction and Figure 4 (b) shows the top section of the RVE. The applied loads of the RVE are assumed to be the same as the ones acting on the test sample.

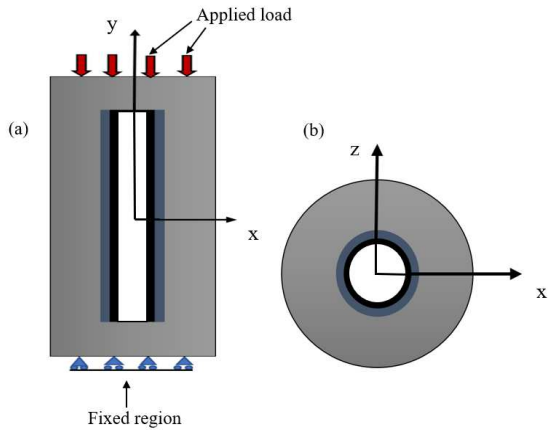

Fig. 4. The RVE with the applied loads on it

The elastic modulus of SWCNT, intermediate phase, and HDPE matrix presented in the RVE is demonstrated in Table 1. The properties and the dimensions of SWCNT and the intermediate phase in Table 1 were obtained from the results of Fattahi et al, [17]. The dimensions of the RVE vary with the x parameter presented in the last column of Table 1.

TABLE I. THE DIMENSIONS AND THE PROPERTIES OF HDPE/SWCNT NANOCOMPOSITES RVE [17, 5]

Properties	SWCNTs (Fiber)	Intermediate phase	HDPE (Matrix)
Initial height (nm)	150	150	Change with x
Outer radius (nm)	5	5.4	Change with x
Internal radius (nm)	4.6	5	Change with x
Elastic Modulus	200 (GPa)	4.06 (GPa)	581.189 (MPa)

To determine the dimensions of RVE, methods from [17, 5] were applied. The dimensions of the x parameter of the RVE presented in Figure 5 depend on the weight fractions of the nanoparticle. Based on the procedure and the model of the calculated x parameter of the RVE, the obtained results are presented in Table 2.

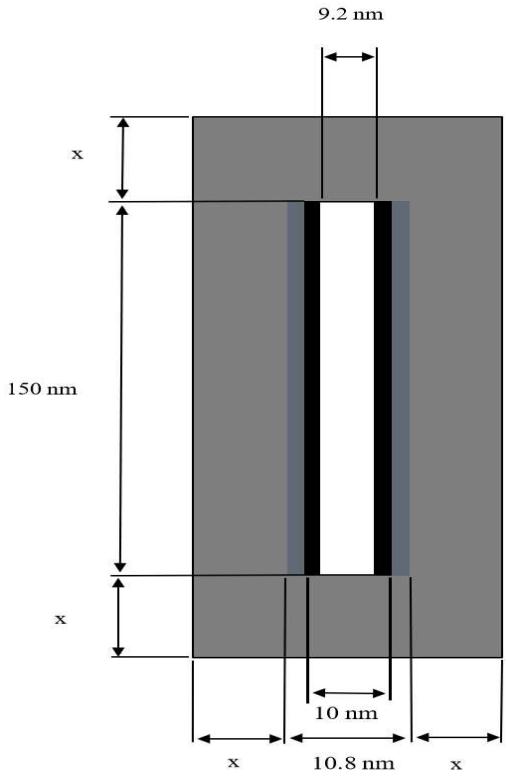

Fig. 5. RVE with the X parameter dimensions

TABLE II. THE OBTAINED X-PARAMETER DEPENDS ON THE SWCNTS WEIGHT FRACTIONS

SWCNTs weight fractions [wt%]	Parameter x (nm)	RVE diameter (nm)	RVE height (nm)
0.2	41.90	94.60	233.80
0.4	29.99	70.78	209.98
0.6	24.33	59.46	198.66
0.8	20.87	52.54	191.84

Based on the obtained properties and the dimensions of the presented RVE, the Finite Element Method (FEM) was applied to predict the displacement U (the depth of the indentation) of the RVE according to the applied loads.

B. *Theoretical FEM*

The Finite Element Method (FEM) was conducted using RVE which is assumed as a body in which the distribution of unknown variables such as the displacement and reaction forces are required. The steps to determine the unknowns were adopted from the FEM approach of [18] as outlined below. The RVE was divided into sections called elements. These elements are connected by nodes at the joints. The assigned variables or the unknowns are assumed to act over each element in a predefined manner. To sufficiently approximate, the variable distribution by combined elemental representations through the whole body of the RVE, the number, and type of element was chosen. After the choice of the elements and their numbers, the governing equations for each element were calculated and then assembled to give the general system equations for each element.

To generate the general solution for the displacement and the reaction force, the concept of the 1-dimensional (1D) springform was adopted according to Equation (1) [18].

$$F = ku \tag{1}$$

Where *F* is the applied force, and *u* is the displacement of the spring of stiffness *k*.

Equation (1) is related to the concept of the Rockwell hardness test utilizing the developed RVE. The RVE of the HDPE matrix in Figure 5 at SWCNT weight fractions according to parameter x in Table 2 will serve as a body where forces are applied. To determine RVE displacement and the resulting force, Equation (2) was applied.

$$\{F\} = [K]\{U\} \tag{2}$$

Where $\{F\}$ is a vector of applied forces at the nodes, $[K]$ is the assembled system stiffness matrix, and $\{U\}$ is the vector of the unknown displacements at the nodes. Equation (2) was applied in the determination of maximum displacement according to Figure 6. Figure 6 (a) presents the pure HDPE with the applied force F and a fixed region. Where applied force F is the indenter load on the RVE which is negative since it is applied as a compression. The fixed region is the resultant force R and the displacements at regions 1 and 2 are denoted by u_1 and u_2, respectively. Figure 6 (b) illustrates the nodes and the element of pure HDPE RVE. Where node 1 is the fixed region, node 2 is where the force is applied. Figure 6 (b) shows that the RVE of pure HDPE has 2 nodes and 1 element which are presented in Table 3.

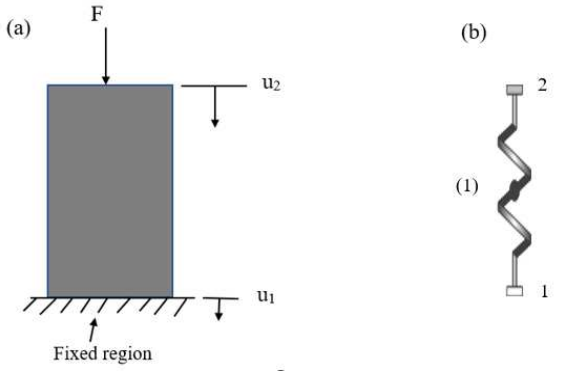

Fig. 6. 1-dimensional (1D) elemental representation of pure HDPE RVE

TABLE III. INITIAL AND FINAL NODES OF ELEMENT 1

Element	i-node	j-node
1	1	2

For the determination of the stiffness matrix for element (1) in Figure 6 (b) of pure HDPE the stiffness matrix in Equation (2) was resolved as:

$$[K] = \frac{A_m E_m}{H_m}\begin{bmatrix} 1 & -1 \\ -1 & 1 \end{bmatrix} \tag{3}$$

Where A_m is the cross-sectional area of the matrix/HDPE RVE, E_m is the elastic modulus of HDPE, and H_m is the height of the HDPE RVE.

Since the cross-sectional area and the height of the RVE vary with parameter x, then the RVE diameter of 0.2 wt% in Table 2 was used to determine the cross-sectional area of pure HDPE RVE as $A_m = 7.029 \times 10^{-9} mm^2$. The height used for pure HDPE was $H_m = 233.80 \times 10^{-6}\, mm$.

$$\frac{A_m E_m}{H_m} = C$$

By letting from Equation (3), we then have the stiffness matrix of one element reduced to:

$$[K] = \begin{bmatrix} C_{11} & -C_{12} \\ -C_{21} & C_{22} \end{bmatrix} \tag{4}$$

Note that $C_{11} = C_{12} = C_{21} = C_{22} = C$ (5)

Where *C* is the term of each element. Equation (4) present the matrix filled by placing the terms of each element stiffness matrix into the correct location.

For the global force vector, the nodal force is:

$$\{F\}^T = [0 \quad -F] \tag{6}$$

Where *F* is the applied force at node 2.

The global deflection and nodal deflection at nodes 1 and 2 are:

$$\{U\}^T = [u_1 \quad u_2] \tag{7}$$

Where *U* is the deflection per node.

The final system equation is presented by substituting Equations (4), (6), and (7) into Equation (2) as:

$$\begin{Bmatrix} 0 \\ -F \end{Bmatrix} = \begin{bmatrix} C_{11} & -C_{12} \\ -C_{21} & C_{22} \end{bmatrix}\begin{Bmatrix} u_1 \\ u_2 \end{Bmatrix} \tag{8}$$

Based on the boundary conditions applied to the generated system Equation (8) according to the RVE in Figure 6. Node point 1 is fixed, therefore, $u_1 = 0$, where the reaction force exists at node 1 which is represented as R_1. Then the general system Equation (8) is modified as:

$$\begin{Bmatrix} R_1 \\ -F \end{Bmatrix} = \begin{bmatrix} C_{11} & -C_{12} \\ -C_{21} & C_{22} \end{bmatrix}\begin{Bmatrix} 0 \\ u_2 \end{Bmatrix} \tag{9}$$

The solution of the system Equation (9) yields the deflection at nodal point 2 which is the maximum deflection and the reaction force at node point 1 as:

$$u_2 = \frac{-F}{C_{22}} \tag{10}$$

$$R_1 = (-C_{12})\frac{-F}{C_{22}} = F \tag{11}$$

For the general solution/system equation for RVE of HDPE reinforced at various weight fractions, the stiffness matrices are generated according to Figure 7. Figure 7 (a) represents the applied forces and the possible displacements that may take place on the HDPE/SWCNTs nanocomposites RVE. Figure 7 (b) presents the nodes and elements generated from Figure 7 (a). It shows that the RVE of reinforced HDPE has 4 nodes and 5 elements. According to the assumptions made in Figure 7 (b), element (1) is the HDPE matrix between nodes 1 and 2 which is the same as element (5) which is between nodes 3 and 4; element (2) is the HDPE matrix parallel to the intermediate phase and SWCNT fiber between nodes 2 and 3; element (3) is the intermediate phase and element (4) is the SWCNT fiber where the applied force F is acting at node 4, the resultant force R is acting at node 1 and the maximum displacement can be obtained at node 4. The elements initial and final nodes of Figure 7 (b) are summarized in Table 4.

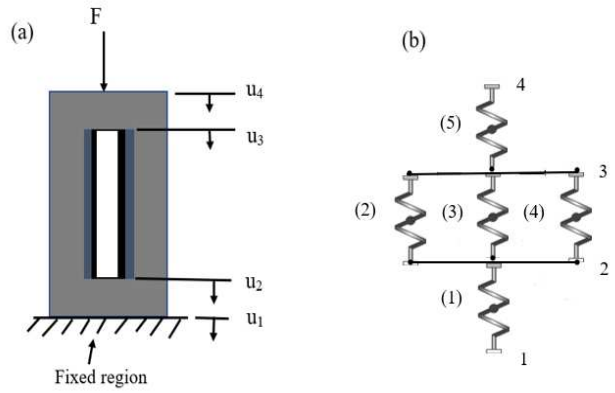

Fig. 7. 1-dimensional (1D) elemental representation of HDPE/SWCNT nanocomposites RVE

TABLE IV. THE INITIAL AND FINAL NODES FOR EACH ELEMENT OF HDPE/SWCNTS NANOCOMPOSITES RVE

Element	i-node	j-node
1	1	2
2	2	3
3	2	3
4	2	3
5	3	4

Since HDPE/SWCNT nanocomposites RVE is represented by five elements and four nodes as shown in Table 4, then the system equation to be generated will contain five stiffness matrices which are: $[K^{(1)}]$, $[K^{(2)}]$, $[K^{(3)}]$, $[K^{(4)}]$, and $[K^{(5)}]$ for each element.

Element (1) represents the HDPE matrix of the RVE which is characterized by the stiffness matrix $[K^{(1)}]$ and it is written as:

$$[K^{(1)}] = \frac{A_{x,m}^{(1)} E_m^{(1)}}{H_{x,m}^{(1)}} \begin{bmatrix} 1 & -1 \\ -1 & 1 \end{bmatrix} \tag{12}$$

According to Equation (12), $A_{x,m}^{(1)}$ is the cross-sectional area of HDPE/SWCNTs nanocomposites RVE represented in Figure 7, $E_m^{(1)}$ is the elastic modulus of HDPE, and $H_{x,m}^{(1)}$ is the height of the HDPE/SWCNTs nanocomposites RVE. The values of $A_{x,m}^{(1)}$ and $H_{x,m}^{(1)}$ depends on the calculated X parameter in Table 2 for each stated SWCNTs weight fraction.

$$[K^{(1)}] = [K^{(5)}] \text{ since } A_{x,m}^{(1)} = A_{x,m}^{(5)},\ E_m^{(1)} = E_m^{(5)} \text{ and } H_{x,m}^{(1)} = H_{x,m}^{(5)} \tag{13}$$

By letting $\frac{A_{x,m}^{(1)} E_m^{(1)}}{H_{x,m}^{(1)}} = \frac{A_{x,m}^{(5)} E_m^{(5)}}{H_{x,m}^{(5)}} = C^{(1)} = C^{(5)}$ form Equations (12) and (13), then the stiffness matrix of elements (1) and (5) can be decreased to:

$$[K^{(1)}] = [K^{(5)}] = \begin{bmatrix} C_{11}^{(1)} & -C_{12}^{(1)} \\ -C_{21}^{(1)} & C_{22}^{(1)} \end{bmatrix} = \begin{bmatrix} C_{11}^{(5)} & -C_{12}^{(5)} \\ -C_{21}^{(5)} & C_{22}^{(5)} \end{bmatrix} \tag{14}$$

Note that:

$$C^{(1)} = C_{11}^{(1)} = C_{12}^{(1)} = C_{21}^{(1)} = C_{22}^{(1)} = C_{11}^{(5)} = C_{12}^{(5)} = C_{21}^{(5)} = C_{22}^{(5)} \tag{15}$$

The stiffness matrix for element (2) is represented as follows:

$$[K^{(2)}] = \frac{A_{x,m}^{(2)} E_m^{(2)}}{H_{x,m}^{(2)}} \begin{bmatrix} 1 & -1 \\ -1 & 1 \end{bmatrix} \tag{16}$$

Where $A_{x,m}^{(2)}$ is the cross-sectional area of HDPE/SWCNTs nanocomposites RVE at element (2) and depends on the calculated *X* parameter in Table 2, $E_m^{(2)}$ is the elastic modulus of HDPE, and $H_{x,m}^{(2)}$ is the height of the HDPE/SWCNTs nanocomposites RVE at element (2) and depending on the *X* parameter which is parallel to the intermediate phase region and the reinforcement. Therefore, $H_{x,m}^{(2)} = H_I = H_f$. Whereby H_I and H_f are the heights of intermediate phase and fiber/reinforcement, respectively.

$\frac{A_{x,m}^{(2)}E_m^{(2)}}{H_{x,m}^{(2)}} = C^{(2)}$ By letting from Equation (16). Then the stiffness matrix for element (2) can be reduced to:

$$[K^{(2)}] = \begin{bmatrix} C_{11}^{(2)} & -C_{12}^{(2)} \\ -C_{21}^{(2)} & C_{22}^{(2)} \end{bmatrix} \quad (17)$$

Where $C^{(2)} = C_{11}^{(2)} = C_{12}^{(2)} = C_{21}^{(2)} = C_{22}^{(2)}$ (18)

The stiffness matrix for element (3) is represented as follows:

$$[K^{(3)}] = \frac{A_I^{(3)}E_I^{(3)}}{H_I^{(2)}} \begin{bmatrix} 1 & -1 \\ -1 & 1 \end{bmatrix} \quad (19)$$

Where $A_I^{(3)}$ is the cross-sectional area of the intermediate phase in HDPE/SWCNTs nanocomposites RVE, $E_I^{(3)}$ is the elastic modulus in the intermediate phase, and $H_I^{(3)}$ is the height of the intermediate phase.

$\frac{A_I^{(3)}E_I^{(3)}}{H_I^{(3)}} = C^{(3)}$ By letting form Equation (19). Then the stiffness matrix for element (3) can be reduced to:

$$[K^{(3)}] = \begin{bmatrix} C_{11}^{(3)} & -C_{12}^{(3)} \\ -C_{21}^{(3)} & C_{22}^{(3)} \end{bmatrix} \quad (20)$$

Where $C^{(3)} = C_{11}^{(3)} = C_{12}^{(3)} = C_{21}^{(3)} = C_{22}^{(3)}$ (21)

The stiffness matrix for element (4) is presented as follows:

$$[K^{(4)}] = \frac{A_f^{(4)}E_f^{(4)}}{H_f^{(2)}} \begin{bmatrix} 1 & -1 \\ -1 & 1 \end{bmatrix} \quad (22)$$

Where $A_f^{(4)}$ is the cross-sectional area of the fibre/SWCNT in HDPE/SWCNTs nanocomposites RVE, $E_f^{(4)}$ is the elastic modulus of the fibre/SWCNT, and $H_f^{(4)}$ is the height of the fibre/SWCNT.

$\frac{A_f^{(4)}E_f^{(4)}}{H_f^{(4)}} = C^{(4)}$ By letting form Equation (22). Then the stiffness matrix for element three can be reduced to:

$$[K^{(4)}] = \begin{bmatrix} C_{11}^{(4)} & -C_{12}^{(4)} \\ -C_{21}^{(4)} & C_{22}^{(4)} \end{bmatrix} \quad (23)$$

Where $C^{(4)} = C_{11}^{(4)} = C_{12}^{(4)} = C_{21}^{(4)} = C_{22}^{(4)}$ (24)

To solve the general system equation, first, we look at the elements that have common nodes. Table 4 shows that elements (2), (3), and (4) have the same i-nodes and j-nodes which are nodes 1 and 2. It also showed that element (1) shares node 2 with element (2) and element (4) shares node 3 with element (5). For a general solution, we start by adding the stiffness matrix 2,3, and 4 since they have common nodes.

The stiffness matrix for elements with the same nodes is calculated as:

$$\sum[K^{(2,3,4)}] = [K^{(2)}] + [K^{(3)}] + [K^{(4)}] \quad (25)$$

$$\sum[K^{(2,3,4)}] = \begin{bmatrix} C_{11}^{(2)} & -C_{12}^{(2)} \\ -C_{21}^{(2)} & C_{22}^{(2)} \end{bmatrix} + \begin{bmatrix} C_{11}^{(3)} & -C_{12}^{(3)} \\ -C_{21}^{(3)} & C_{22}^{(3)} \end{bmatrix} + \begin{bmatrix} C_{11}^{(4)} & -C_{12}^{(4)} \\ -C_{21}^{(4)} & C_{22}^{(4)} \end{bmatrix} \quad (26)$$

$$\sum[K^{(2,3,4)}] = \begin{bmatrix} \sum C_{11}^{(2,3,4)} & -\sum C_{12}^{(2,3,4)} \\ -\sum C_{21}^{(2,3,4)} & \sum C_{11}^{(2,3,4)} \end{bmatrix} \quad (27)$$

Equation (27) represents the stiffness matrix of elements (2), (3), and (4) whereby.

$$\sum C_{11}^{(2,3,4)} = C_{11}^{(2)} + C_{11}^{(3)} + C_{11}^{(4)} \quad (28)$$

$$-\sum C_{12}^{(2,3,4)} = -C_{12}^{(2)} - C_{12}^{(3)} - C_{12}^{(4)} \quad (29)$$

$$-\sum C_{21}^{(2,3,4)} = -C_{21}^{(2)} - C_{21}^{(3)} - C_{21}^{(4)} \quad (30)$$

$$\sum C_{22}^{(2,3,4)} = C_{22}^{(2)} + C_{22}^{(3)} + C_{22}^{(4)} \quad (31)$$

We have

$$\sum C_{11}^{(2,3,4)} = \sum C_{12}^{(2,3,4)} = \sum C_{21}^{(2,3,4)} = \sum C_{22}^{(2,3,4)} \quad (32)$$

Therefore, the stiffness matrix $[K]$ for the general equation of HDPE/SWCNTs nanocomposites and various weight fractions of SWCNTs nanoparticles can be represented as follows:

$$[K] = \begin{bmatrix} C_{11}^{(1)} & -C_{12}^{(1)} & 0 & 0 \\ -C_{21}^{(1)} & C_{22}^{(1)} + \sum C_{11}^{(2,3,4)} & -\sum C_{21}^{(2,3,4)} & 0 \\ 0 & -\sum C_{21}^{(2,3,4)} & \sum C_{22}^{(2,3,4)} + C_{11}^{(5)} & -C_{12}^{(5)} \\ 0 & 0 & -C_{21}^{(5)} & C_{22}^{(5)} \end{bmatrix} \quad (33)$$

Note from equation (33):

$$C_{22}^{(1)} + \sum C_{11}^{(2,3,4)} = \sum C^{(1,2,3,4)} \quad (34)$$

$$\sum C_{22}^{(2,3,4)} + C_{11}^{(5)} = \sum C^{(2,3,4,5)} \quad (35)$$

$$\sum C^{(1,2,3,4)} = \sum C^{(2,3,4,5)} \quad (36)$$

Equations (34) and (35) were obtained for the analogy stating that element (1) shares node 2 with element (2) and element (4) shares node 3 with element 5. Meaning that row 2 and column 2 of the stiffness matrix 2 should be added to row 1 and column 1 of the stiffness matrix 2,3, and 4. Again row 2 and column 2 of stiffness matrices 2,3, and 4 should be added to row 1 and column 1 of stiffness matrix 5. Therefore, the simplified form of the general stiffness matrix is presented as:

$$[K] = \begin{bmatrix} C_{11}^{(1)} & -C_{12}^{(1)} & 0 & 0 \\ -C_{21}^{(1)} & \sum C^{(1,2,3,4)} & -\sum C_{21}^{(2,3,4)} & 0 \\ 0 & -\sum C_{21}^{(2,3,4)} & \sum C^{(1,2,3,4)} & -C_{12}^{(1)} \\ 0 & 0 & -C_{21}^{(1)} & C_{11}^{(1)} \end{bmatrix} \quad (37)$$

The global force vector for the general solution, nodal force is:

$$\{F\}^T = [0 \quad 0 \quad 0 \quad -F] \quad (38)$$

Where F is the applied force at node 4

The global deflection and nodal deflection at nodes 1 and 2 are:

$$\{U\}^T = [u_1 \quad u_2 \quad u_3 \quad u_4] \quad (39)$$

The final system equation of HDPE reinforced at different weight fractions of SWCNTs nanoparticles is presented by substituting Equations (37), (38), and (39) into Equation (2) as:

$$\begin{Bmatrix} 0 \\ 0 \\ 0 \\ -F \end{Bmatrix} = \begin{bmatrix} C_{11}^{(1)} & -C_{12}^{(1)} & 0 & 0 \\ -C_{21}^{(1)} & \sum C^{(1,2,3,4)} & -\sum C_{21}^{(2,3,4)} & 0 \\ 0 & -\sum C_{21}^{(2,3,4)} & \sum C^{(1,2,3,4)} & -C_{12}^{(1)} \\ 0 & 0 & -C_{21}^{(1)} & C_{11}^{(1)} \end{bmatrix} \begin{Bmatrix} u_1 \\ u_2 \\ u_3 \\ u_4 \end{Bmatrix} \quad (40)$$

Based on the boundary conditions applied to the generated system Equation (40) according to the RVE in Figure 7. The node point 1 is fixed, therefore, $u_1 = 0$, where the reaction force exists at node 1 which is represented as R_1. Then the general system Equation (40) is modified as:

$$\begin{Bmatrix} R_1 \\ 0 \\ 0 \\ -F \end{Bmatrix} = \begin{bmatrix} C_{11}^{(1)} & -C_{12}^{(1)} & 0 & 0 \\ -C_{21}^{(1)} & \sum C^{(1,2,3,4)} & -\sum C_{21}^{(2,3,4)} & 0 \\ 0 & -\sum C_{21}^{(2,3,4)} & \sum C^{(1,2,3,4)} & -C_{12}^{(1)} \\ 0 & 0 & -C_{21}^{(1)} & C_{11}^{(1)} \end{bmatrix} \begin{Bmatrix} 0 \\ u_2 \\ u_3 \\ u_4 \end{Bmatrix} \quad (41)$$

Equation (41) represents the general system equation that can be applied to determine the maximum deflections of reinforced HDPE at different weight fractions. The solution of the general system Equation (41) yields the reaction force at node point 1 deflection at nodes 2, 3,4, and 5. Where the deflection at point 5 is the maximum. The general solutions of the deflection and the reaction force are:

$$u_2 = \frac{-F}{C_{12}^{(1)}} \quad (42)$$

$$u_3 = \frac{-F\sum C^{(1,2,3,4)}}{\left(C_{12}^{(1)}\right)^2} \quad (43)$$

$$u_4 = \frac{-F\left(\frac{\left(\sum C^{(1,2,3,4)}\right)^2}{\sum C_{12}^{(2,3,4)}} - \sum C_{21}^{(2,3,4)}\right)}{\left(C_{12}^{(1)}\right)^2} \quad (44)$$

$$R_1 = \left(-C_{12}^{(1)}\right)\frac{-F}{C_{12}^{(1)}} = F \quad (45)$$

The FEM results for the generated general system equation are presented and discussed in section 4.

III. Materials and Methods

A. Materials

The materials used for this investigation are High-Density Polyethylene (HDPE), Single-wall Carbon Nanotubes (SWCNTs), and Maleic anhydride. The material properties and mixing technique used are as stated in the paper by Tebeta et al, [5].

B. Methods

The synthesis and the processing of HDPE/SWCNTs nanocomposites at various weight fractions of SWCNTs were carried out according to Tebeta et al, [5]. Where maleic anhydride was used to disperse the SWCNTs nanoparticles through the HDPE matrix. The weight fractions of SWCNTs varied from 0 wt% to 0.8 wt% with an increment of 0.2. The Charpy impact test samples were processed according to the ASTM standard D256 – 04 [19]. The dimensions of the test samples are given as: 63.5 $\pm$ 2.0 mm in length, a width of 12.70 $\pm$ 0.20 mm, a thickness of 3.5 mm, a V notch depth of 2.5, and an angle of 45 degrees.

The V-notch Charpy impact test samples produced at various weight fractions of SWCNTs are presented in Figure 8.

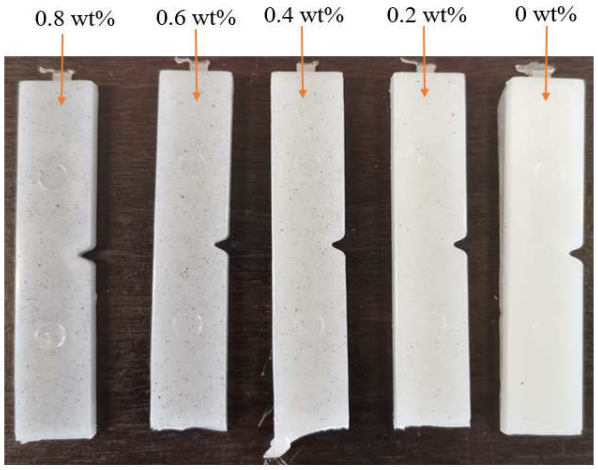

Fig. 8. HDPE/SWCNTs nanocomposites impact test specimen before testing

C. *Examination and measurements*

The produced HDPE/SWCNTs nanocomposites were examined through the Charpy impact and hardness test. The Charpy impact test was performed to determine the energy absorbed during the swinging of the testing pendulum. The test was conducted using an impact testing machine presented in Figure 9 conforming to the ASTM test standard D6110-10 [19]. The Charpy impact testing machine used is shown in Figure 9.

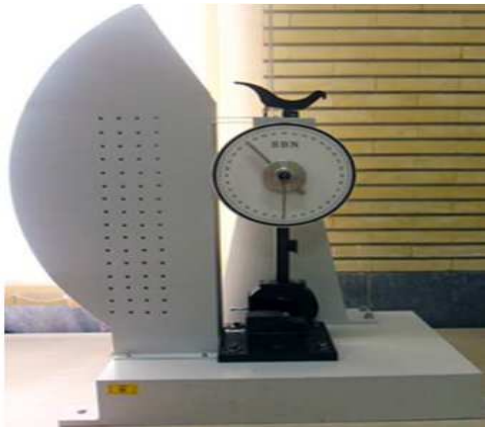

Fig. 9. Impact testing machine

The initial operating parameters of the machine were set as follows: the rise angle of 150.100 degrees and potential energy of 248.56 J. Initially the impact test machine pendulum was let swing with no test specimen and the rise angle of the pendulum was recorded to be -150.100 degrees for the first swing on the other side of the pendulum past the test section. The process was repeated three times and the average absorbed energy was found to be 0.00 J. these readings were taken as the initial reading for the calibration. The rise angle was constant for all the tests. The impact test was then conducted for all HDPE/SWCNTs nanocomposites samples where their test was made for each weight fraction and the average results were recorded according to Tables 6 and 7. The remaining pieces of the V-notch Charpy impact test samples were used for hardness testing. The hardness test was conducted using a digital/universal hardness tester machine model 570HAD as shown in Figure 10.

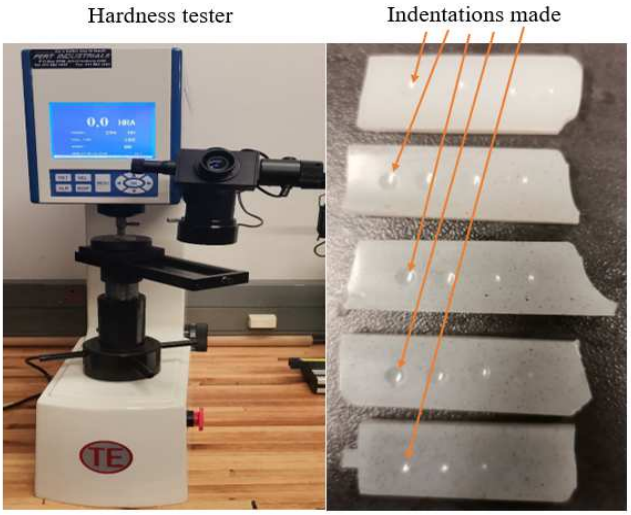

Fig. 10. Hardness testing machine

The technical specifications of the hardness testing machine HBRV – 187.5D were set to Rockwell Scales HRB. The hardness Rockwell B (HRB) scale uses the 1.588mm diameter ball indenter and the test load of 100 kg. The stated test parameter was set for a dwell time of 10 seconds and the HRB values were automatically converted to the HV values. Four indentations were made on each sample and the average results were recorded in Tables 8 and 9. The experimental results of the Charpy impact test and the hardness results are discussed in the next section.

IV. RESULTS AND DISCUSSIONS

A. *Theoretical FEM Results*

The results of the maximum displacement for pure HDPE (0 wt%) and the reinforced HDPE at (0.2 wt%, 0.4 wt%, 0.6 wt%, and 0.8 wt%) are obtained independently using the system Equations (9) and (41), respectively. The results for pure HDPE were obtained by using the stated cross-sectional area and height RVE in Figure 6 and the elastic modulus of HDPE from Table 1. The stated parameter was substituted in Equation (9) and the maximum displacement, and the presented force was determined using Equations (10) and (11), respectively. For HDPE at various weight fractions, cross-sectional areas of the HDPE matrix were determined in terms of RVE parameter x depending on SWCNT weight fraction as illustrated in Table 2. The intermediate phase and SWCNT cross-sectional areas were calculated using the dimensions in Table 2. The results obtained are summarized in Table 5.

TABLE V. MAXIMUM DISPLACEMENTS OF HDPE AND REINFORCED HDPE RVE

SWCNTs Weight Fractions [wt%]	**Maximum displacement** $(\times 10^{-6})$ **[mm]**	**Positive Maximum displacement** $(\times 10^{-6})$ **[mm]**
0	-192.22	192.22
0.2	-153.20	153.20
0.4	-114.17	114.17
0.6	-93.59	93.59
0.8	-73.24	73.24

The results in Table 5 show that the displacements U decrease as the weight fraction of SWCNTs nanoparticles increases. This shows that the addition of SWCNTs nanoparticles into the HPDE matrix toughens the nanocomposites. This correlates with the statement made stating that if the material is hard, the depth of indentation is low. This shows that the addition of the weight fraction of SWCNTs nanoparticles results in the harder HDPE/SWCNTs nanocomposites.

B. Charpy Impact Test Results

Pure HDPE of 0 wt% of SWCNTs and HDPE/SWCNTs nanocomposites at the weight fractions of 0.2 wt%, 0.4 wt%, 0.6 wt%, and 0.8 wt% were processed according to injection molding as mentioned. Their impact energy properties were examined, and the results obtained are shown in the following tables.

Table 6 presents the obtained values of energy absorbed during the impact of the pendulum and the test samples. For each weight fraction of SWCNTs nanoparticles, three tests were made, and the average absorbed energy was recorded. The average value is assumed to be more representative of the general value of absorbed energy.

TABLE VI. CHARPY IMPACT TEST ABSORBED ENERGY RESULTS

Sample Number	**SWCNTs Weight Fractions [wt%]**	**Absorbed Energy [J]**			**Average Absorbed Energy [J]**
		Test 1	***Test 2***	***Test 3***	
1	0	0.79	0.76	0.79	0.78
2	0.2	1.07	1.05	1.08	1.07
3	0.4	1.11	1.09	1.12	1.11
4	0.6	1.20	1.15	1.18	1.18
5	0.8	1.29	1.27	1.25	1.27

From Table 6, Figure 11 was generated to demonstrate the relationship between the weight fraction of SWCNTs nanoparticles and the average energy absorbed. The relationship in Figure 11 shows that an increase in SWCNTs weight fractions in the HDPE matrix is directly proportional to the average absorbed energy. This means the addition of SWCNTs weight fractions strengthens/toughen the HDPE matrix. The Charpy impact test demonstrated that unreinforced HDPE (pure HDPE with 0 wt% of SWCNTs) absorbed less average energy compared to those reinforced at the weight fractions of 0.2 wt% to 0.8 wt%. Furthermore, it was shown through the digital display screen on the computer connected to the impact tester that, the pendulum at the initial angle of 150.100 degrees raised to an angle of -149.450 degrees after the impact. This shows that a small amount of energy was absorbed that reduced the rise angle after the impact from 150.100 degrees to 149.450 degrees. The results of the decrease in rising angle after the impact of the pendulum at the given weight fractions of the test samples are presented in Table 7.

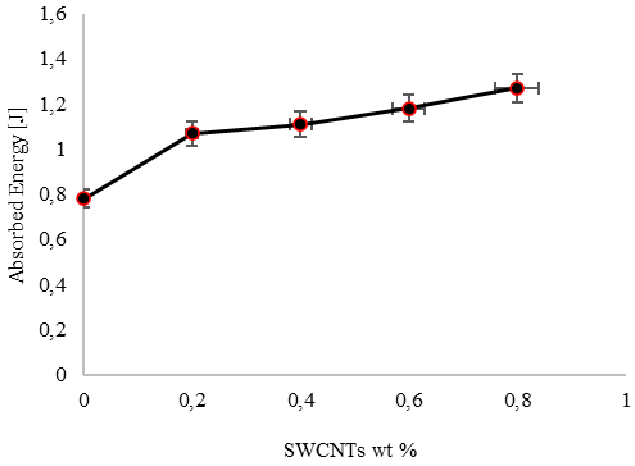

Fig. 11. Average energy absorbed against SWCNTs weight fractions

Table 7 demonstrates the effect of strengthened/reinforced HDPE/SWCNTs nanocomposites and the average absorbed energy, potential energy, and the rise angle of the pendulum after the impact. According to the concept of the Charpy impact test, the test sample serves as an obstacle to the swinging pendulum. If there is no test sample, the pendulum should swing to the initial rise angle after the test section. However, if there is a test sample, an amount of kinetic energy will be absorbed from the swinging pendulum depending on the hardness or strength of the material. The stronger the material the more kinetic energy absorbed, the weaker the material, the lesser the kinetic energy absorbed. From this idea of impact energy, it is shown in Tables 6 and 7 as well as in Figure 11 that HDPE/SWCNTs nanocomposites with SWCNTs weight fraction of 0.8 wt% absorbed 1.27 J average energy compared to 0.78 J average energy absorbed by pure HDPE of 0 wt%. This shows that HDPE/SWCNTs nanocomposites at 0.8 wt% of SWCNTs have been strengthened by 62.8% compared to pure HDPE at 0 wt%.

TABLE VII. THE RISE ANGLE OF THE PENDULUM AFTER THE IMPACT WITH THE HDPE/SWCNTs NANOCOMPOSITES TEST SAMPLES

SWCNTs weight fractions [wt%]	**Rise Angle [^{0}]**	**Potential Energy [J]**	**Compensated Energy [J]**
0	-149.450	249.00	0.07
0.2	-149.200	248.71	0.24
0.4	-149.175	248.68	0.28
0.6	-149.100	248.56	0.33
0.8	-149.078	248.51	0.42

After the Charpy impact test, the remaining pieces of HDPE/SWCNTs nanocomposites test samples were collected and some of them were used for the hardness testing. Figure 12 shows some of the collected parts of the test specimen. It is demonstrated in Figure 12 that the sample broke apart after the test which means they are brittle. For the validation of the brittle properties of the samples. The tensile test result of Tebeta et al, [5], was used.

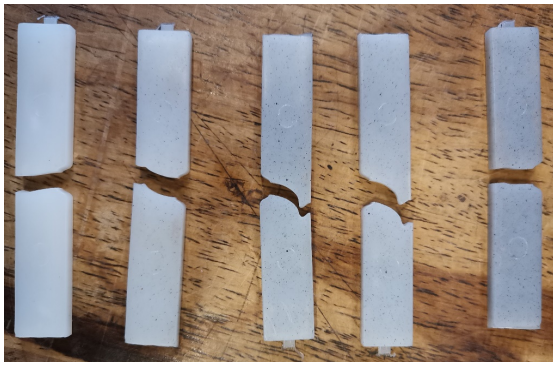

Fig. 12. Pure HDPE and HDPE/SWCNTs nanocomposites samples after the impact test

Figure 13 illustrates the stress-strain curve of the tensile test results of Tebeta et al, [5]. From the stress-strain curves of HDPE/SWCNTs nanocomposites in Figure 13 shows that tensile test samples fractured without elongating further to the plastic deformation region. According to ISO 527, [20] and ASTM D638 – 02a, [21] standards, the stress-strain curve presented in Figure 13 represent the characteristics of strong and brittle materials which deformed elastically and then failed. The impact test results, and the tensile test results correspond to each other by showing that the tested HDPE/SWCNTs nanocomposites samples are brittle.

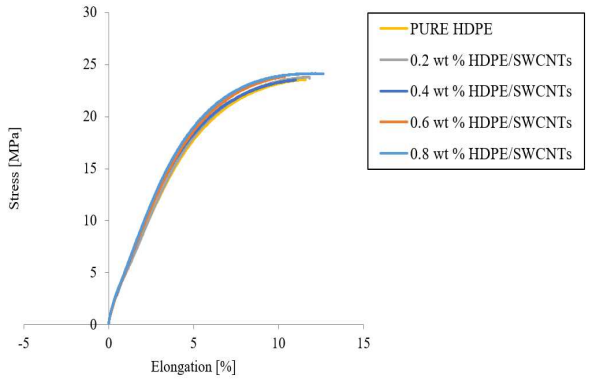

Fig. 13. Stress-strain curves of HDPE/SWCNTs nanocomposites at various weight fractions

Although it has been demonstrated by the Charpy impact test and tensile test that the reinforced HDPE at different weight fractions of SWCNTs is strong and brittle. A further experiment on the hardness properties of the produced nanocomposites was conducted and the results are discussed in the next section.

C. *Hardness Test Results*

The hardness test was conducted using the remaining pieces of the pure and reinforced HDPE from the Charpy impact test. For each sample used four indentations were made and their average was taken as illustrated in Tables 8 and 9.

TABLE VIII. HRB HARDNESS TEST RESULTS

Sample Number	SWCNTs Weight Fractions [wt%]	Hardness (Rockwell HRB)				Average (Rockwell HRB)
		Test 1	*Test 2*	*Test 3*	*Test 4*	
1	0	59.9	58.3	59.2	61.9	59.8
2	0.2	62.4	63.6	62.2	62.8	62.8
3	0.4	64.6	66.0	63.8	63.7	64.5
4	0.6	68.5	67.9	69.	66.8	68.1
5	0.8	69.9	74.1	73.2	69.2	71.6

TABLE IX. HRB HARDNESS TEST RESULTS CONVERTED TO HV

Sample Number	SWCNTs Weight Fractions [wt%]	Hardness (Rockwell HV)				Average (Rockwell HV)
		Test 1	*Test 2*	*Test 3*	*Test 4*	
1	0	107	105	106	110	107
2	0.2	111	113	110	112	112
3	0.4	115	117	114	113	115
4	0.6	122	121	124	119	122
5	0.8	125	135	133	123	129

The hardness test results in Table 9 show that the average Rockwell HV of the HDPE/SWCNTs nanocomposites tested samples increase as the weight fraction of SWCNTs nanoparticles increases. This implied that the hardness properties of the processed polymer-based nanocomposites improve with the addition of nanoparticle weight fraction. The hardness properties of HDPE/SWCNTs nanocomposites at 0.8 wt% of SWCNTs nanoparticles have improved by 20.6% compared to pure HDPE at 0 wt%. The overall results of the tensile test, impact test, and hardness test showed that HDPE/SWCNTs nanocomposites retain hard, tough, and brittle properties. Although is not always the case that every polymer-based nanocomposite will possess the same properties. The main influence on such properties is the parameters and the processing techniques used to produce the material. For example, the processing temperature of melting the plastic or the cooling rate determines if the product will be ductile or brittle. The reinforcing nanoparticles determine the strength and the thermal properties of the produced polymer-based nanocomposites. It is possible to achieve different tensile, impact strength, or hardness properties of HDPE/SWCNTs nanocomposites from the one presented in this paper. The reasons are the processing method used, processing parameters, and the experimental testing conditions and limitations.

V. CONCLUSIONS

In this study, High-Density Polyethylene-Single-Walled Carbon Nanotubes nanocomposites (HDPE/SWCNTs) were produced according to the injection molding. The effect of adding SWCNTs nanoparticles at 0 wt% to 0.8 wt% with the increment of 0.2 on the impact strength and hardness of

HDPE/SWCNTs nanocomposites samples was investigated. The results obtained showed the following:

- The addition of 0.8 wt% SWCNTs into the HDPE matrix increased the impact strength and hardness properties of the samples significantly by 62.8 % and 20.6 % respectively.
- The processed samples proved to get tougher, and more brittle as the weight fraction of SWCNTs nanoparticles increased.
- The theoretical FEM hardness results proved to correlate with the experimental hardness test results.

ACKNOWLEDGMENT

The authors wish to acknowledge: The University of South Africa (UNISA) Department of Mechanical Engineering and the University of Johannesburg (UJ)

REFERENCES

[1] D. Tripathy and B. Sahoo, Properties and applications of polymer nanocomposites, GmbH, Germany: Springer-Verlag, 2017.

[2] N. Salah, A. Alfawzan, A. Saeed, A. Alshahrie and W. Allafi, "Effective reinforcements for thermoplastics based on carbon nanotubes of oil fly ash," *Scientific Reports,* vol. 9, no. 1, pp. 1-13, 2019.

[3] M. Rafiee, J. Rafiee, Z. Wang, H. Song, Z. Yu and N. Koratkar, "Enhanced mechanical properties of nanocomposites at low graphene content," *ACS nano,* vol. 3, no. 12, pp. 3884-3890, 2009.

[4] Y. Liu, H. Wu and G. Chen, "Enhanced mechanical properties of nanocomposites at low graphene content based on in situ ball milling," *Polymer Composites,* vol. 37, no. 4, pp. 1190-1197, 2016.

[5] R. Tebeta, A. Fattahi and N. Ahmed, "Experimental and numerical study on HDPE/SWCNT nanocomposite elastic properties considering the processing techniques effect," *Microsystem Technologies,* pp. 1-9, 2020.

[6] S. Thakur, N. Sharma and N. Batra, "Tribological characterization of CNT/HDPE polymer nano-composites," *Int. J. Theor. Appl. Res. Mech. Eng,* vol. 1, pp. 32-36, 2012.

[7] A. Najipour and A. Fattahi, "Experimental study on mechanical properties of PE/CNT Composites," *ournal of Theoretical and Applied Mechanics,* vol. 55, no. 2, pp. 719-726, 2017.

[8] R. Tebeta, A. Ahmed and A. Fattahi, "Experimental study on the effect of compression load on the elastic properties of HDPE/SWCNTs nanocomposites," *Microsystem Technologies,* pp. 1-10, 2021.

[9] M. Rasoolpoor, R. Ansari and M. Hassanzadeh-Aghdam, "Influences of carbon nanotubes on low velocity impact performance of metallic nanocomposite plates–A coupled numerical approach," *Mechanics Based Design of Structures and Machines,* pp. 1-15, 2020.

[10] S. Kamarian, M. Bodaghi, R. Isfahani, M. Shakeri and M. Yas, "Influence of carbon nanotubes on thermal expansion coefficient and thermal buckling of polymer composite plates: Experimental and numerical investigations," *Mechanics Based Design of Structures and Machines,* vol. 49, no. 2, pp. 217-232, 2021.

[11] D. Zhang, M. Ashraf, Z. Liu, C. Li, and W. Peng, "Effect of graphene nanoplatelets addition on the elastic properties of short ceramic fiber-reinforced aluminum-based hybrid nanocomposites," *Mechanics Based Design of Structures and Machines,* pp. 1-17, 2020.

[12] M. Feri, M. Krommer and A. Alibeigloo, "Three-dimensional static analysis of a viscoelastic rectangular functionally graded material plate embedded between piezoelectric sensor and actuator layers.," *Mechanics Based Design of Structures and Machines,,* pp. 1-25, 2021.

[13] M. Al-Furjan, M. Habibi, D. W. Jung, H. Safarpour and M. Safarpour, "On the buckling of the polymer-CNT-fiber nanocomposite annular system under thermo-mechanical loads.," *Mechanics Based Design of Structures and Machines.,* pp. 1-21, 2020.

[14] H. Dehghani, B. Brooksby, K. Vishwanath, B. Pogue and K. Paulsen, "The effects of internal refractive index variation in near-infrared optical tomography: a finite element modelling approach.," *Physics in Medicine & Biology,* vol. 48, no. 16, p. 2713, 2003.

[15] M. Horritt and P. Bates, "Predicting floodplain inundation: raster-based modelling versus the finite-element approach.," *Hydrological processes.,* vol. 15, no. 5, pp. 825-842, 2001.

[16] H. Pollack, Materials science and metallurgy., New Jerey, 07632, USA: Prentice Hall Inc, a division of Simon and Schuster, Englewood Cliffs, 1988.

[17] A. Fattahi, S. Roozpeikar and N. Ahmed, "FEM modeling based on molecular results for PE/SWCNT nanocomposites," *International Journal of Engineering & Technology www. sciencepubco. com/index. php/IJET ,* vol. 7, pp. 1-12, 2018.

[18] M. Fagan, Finite Element Analysis , Theory and Practice, Essex, England.: Longman Scientific and Technical, 1992.

[19] A. International, Writer, *Standard test method for determining the charpy impact resistance of notched specimens of plastics.* [Performance]. American Society for Testing and Materials, 2008.

[20] H. Fahrenholz, "The 2012 version of ISO 527 plastics: determination of tensile properties, Zwick/Roell," 2018.

[21] A. S. D. 10, "Mechanical Properties. Standard test method for tensile properties of thin plastic sheeting. American Society for Testing and Materials," 1995.

[22] A. International, "Standard test method for determining the Charpy impact resistance of notched specimens of plastics, ASTM D6110-10".